A computational fluid dynamic study of stent graft remodeling after endovascular repair of thoracic aortic dissections

Stephen W. K. Cheng, MS,[a] Edward S. K. Lam, MPh,[b] George S. K. Fung, PhD,[c] Pei Ho, MB, BS,[a] Albert C. W. Ting, MS,[a] and **Kwok W. Chow, BS, PhD,[b]** *Hong Kong, China*

Objectives: **Significant stent graft remodeling commonly occurs after endovascular repair of thoracic aortic dissections because of continuing expansion of the true lumen. A suboptimal proximal landing zone, minimal oversizing, and lack of a healthy distal attachment site are unique factors affecting long-term stent graft stability. We used computational fluid dynamic techniques to analyze the biomechanical factors associated with stent graft remodeling in these patients.**

Patients and Methods: **A series of computational fluid dynamic models were constructed to investigate the biomechanical factors affecting the drag force on a thoracic stent graft. The resultant drag force as a net change of fluid momentum was calculated on the basis of varying three-dimensional geometry and deployment positions. A series of 12 patients with type B aortic dissections treated by thoracic stent graft and followed up for more than 12 months were then studied. Computed tomography transaxial images of each patient shortly after stent graft deployment and on subsequent follow-up were used to generate three-dimensional geometric models that were then fitted with a surface mesh. Computational fluid dynamic simulations were then performed on each stent graft model according to its geometric parameters to determine the actual change in drag force experienced by the stent graft as it remodels over time.**

Results: **The drag force on the stent graft model increases linearly with its internal diameter and becomes highest when the deployment position is closer to the proximal arch. Aortic curvature is not a significant factor. Serial computed tomography scans of patients showed an increase in mean inlet area from 1030 mm^2 to 1140 mm^2, and mean outlet area from 586 mm^2 to 884 mm^2 (increase of 11% and 58%, respectively; $P = .05$, .01). These increases are associated with a change in resultant drag force on the stent graft from 21.0 N to 24.8 N (mean increase, 19.5%; range, 0%-63.2%; $P = .002$). There is a positive relationship between increase in drag force and increase in stent-graft area.**

Conclusion: **The drag force on thoracic stent grafts is high. A significant change in stent-graft diameter occurs after endovascular repair for type B dissections, which is associated with an increase in hemodynamic drag force. These stent grafts may be subjected to a higher risk of distal migration, and continuing surveillance is mandatory. (J Vasc Surg 2008; 48:303-10.)**

Endovascular stent grafts placed in the aorta are subjected to significant displacement forces generated by high blood flow. Previous in vivo and computational studies[1,2] on abdominal aortic stent grafts have demonstrated that these forces are higher with a larger graft inlet diameter and can result in distal migration of abdominal stent grafts. Very few studies so far have been done on the hemodynamic forces of thoracic stent grafts.

Thoracic stent grafts are often of a larger diameter and are strategically placed near the aortic arch where there is a substantial element of transverse flow. There are also considerable variations in the length of the stent graft, its deployment position relative to the arch, and the curvature of the aorta. Thoracic stent grafts are predisposed to considerable remodeling after deployment because of the inherent large volume of the grafts. Remodeling is most evident in patients in whom the stent grafts are placed for aortic dissections, in which the changes in true lumen diameter (and therefore stent-graft diameter) can be substantial as the false lumen regresses. Stent grafts deployed in these situations therefore exist in a dynamic state of continuous geometric alterations, and changes in distraction forces can occur, which may affect long-term durability of the repair.

We aimed to (1) study, using computational fluid dynamics (CFD), the forces acting on thoracic stent grafts and their relationship to geometry and flow, and (2) determine the changes in resultant drag forces associated with stent-graft remodeling using three-dimensional (3D) flow models constructed from serial CT scan data in actual patients with stent grafts placed for aortic dissections.

PATIENTS AND METHODS

To perform computational simulation of pulsatile blood flow for a stent graft in the thoracic aorta, three major components are required: (1) geometry, which defines the 3D shape of the stent graft; (2) governing equations, which elucidate the fundamental fluid principles an-

From the Department of Surgery, University of Hong Kong Medical Centre, Queen Mary Hospital,[a] and the Departments of Mechanical Engineering[b] and Electrical and Electronic Engineering,[c] The University of Hong Kong.

Competition of interest: none.

Presented at the Twentieth Annual Meeting of the Western Vascular Society, Kona, Hawaii, Sep 8-11, 2007.

Reprint requests: Stephen W. K. Cheng, Division of Vascular Surgery, Department of Surgery, University of Hong Kong Medical Centre, Queen Mary Hospital, Pokfulam Road, Hong Kong (e-mail: wkcheng@hku.hk).

0741-5214/$34.00

doi:10.1016/j.jvs.2008.03.050

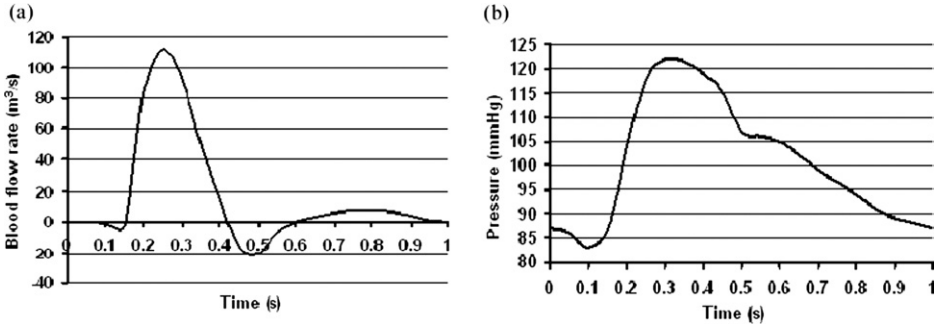

Fig 1. Blood flow waveform **(a)** and blood pressure waveform **(b)**. The period is one second per cycle. Peak flow occurred at 0.25 seconds and peak pressure at 0.3 seconds.

alytically; and (3) boundary conditions, which describe the characteristics of the pulsatile blood flow. The drag force on a stent graft can then be calculated by applying the fundamental principles of fluid mechanics.

Governing equations. Blood flow in large arteries is typically sufficiently fast to justify the assumption that the blood behaves as a Newtonian fluid.[3] The governing principles of the motion of a 3D fluid are the conservation laws of mass and momentum. More precisely, they are the continuity equation

$$\frac{\partial u_i}{\partial x_i} = 0$$

and the Navier-Stokes equations for an incompressible fluid

$$\frac{\partial u_i}{\partial t} + u_j \frac{\partial u_i}{\partial x_j} = -\frac{1}{\rho}\frac{\partial p}{\partial x_i} + \frac{1}{\rho}\frac{\partial \tau_{ij}}{\partial x_j},$$

where u_i ($i = 1, 2, 3$) are the components of the velocity vector, p is the pressure, and ρ is the fluid density. The summation convention is employed.

Boundary conditions. The governing equations are allowed to march forward in time with an established routine and appropriate boundary conditions. The rheological properties are assumed to be in ranges that permit blood to be treated as an incompressible, homogeneous, and Newtonian fluid. This is a reasonable assumption in larger arteries such as the thoracic aorta. With this working assumption, the shear stress in the blood is proportional to the velocity gradient in the blood. The dynamic viscosity of blood, μ, is taken to be 0.0035 Ns/m^2, and 1050 kg/m^3 is the assumed blood density.[4]

Physiologically representative pulsatile velocity waveform and pressure waveform are applied at the inlet and outlet respectively (Fig 1). These velocity profile waveforms are verified in actual patients at the completion of thoracic endograft procedures by taking real-time pressure and waveform readings with a pressure transducer connected to a large-caliber catheter (VOTT; Cook Medical, Bloomington, Ind) placed at the inlet and pulled back at 2-cm intervals. The waveforms used in the simulations are in agreement and have also been verified by various in vivo experimental data.[5,6]

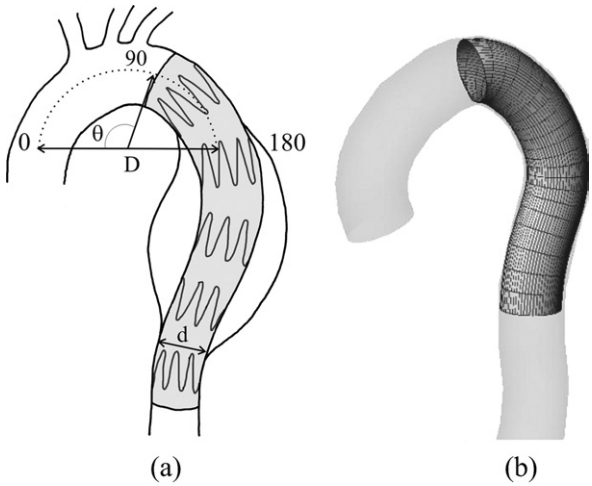

Fig 2. a, Geometric parameters defining the stent graft model. **b,** Surface mesh elements created for the fluid domain. *d*, Diameter of the stent graft; θ, position of deployment of stent graft in clockwise direction from aortic valve; *D*, diameter of curvature of the aortic arch.

The hemodynamic effects of blood plasma only were considered, and the particle effects on the simulation are deemed negligible so as to avoid an excessively high computational workload. In large blood vessels, the fluid flow is treated as laminar for moderate Reynolds numbers.[6,7]

To attain a periodic state in a time-dependent calculation in CFD simulations,[8,9] a steady-state solution at the maximum flow rate is obtained first. Data and output from the fifth cycle are taken as the time-periodic solution. The domain wall boundaries are assumed to be rigid, and the no-slip boundary condition is applied at all vessel walls.

Drag force calculations. Drag force was calculated from direct integration of the pressure and wall shear stress distributions on both surfaces of the stent-graft wall:

$$\sum \mathrm{F} = \int_{C.S.} P \cdot dA + \int_{C.S.} \tau \cdot dA,$$

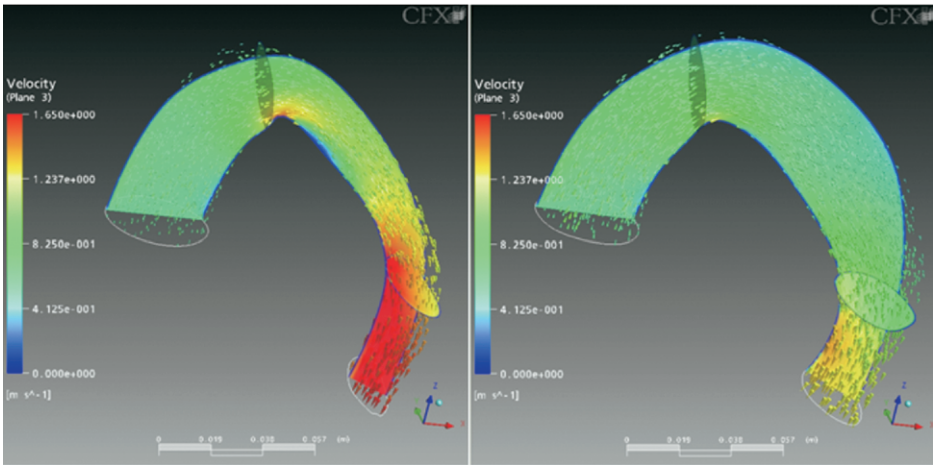

Fig 3. Patient-derived CFX model of fluid dynamics velocity and vector plot in a thoracic stent graft before (*left*) and after (*right*) remodeling.

where F = drag force, P = pressure acting on the stent graft, τ = shear stress acting on the stent graft, and *C.S.* = control surface.

The drag force exerted by the blood flow on the stent-graft wall is mainly generated by two sources: the net change or efflux in fluid momentum and the friction on the graft wall. The net change in fluid momentum contributes the majority of a drag force on the stent graft.[1,7] The net drag force acting on a stent graft induced mainly by the change of momentum in blood flow can be calculated by the momentum theorem from classical fluid mechanics.[10] This theorem states that the total forces acting on a control volume containing fluid will be computed from the net rate of momentum efflux from the control volume, plus the time rate of change of momentum within the control volume. In our study, the latter made only a minor contribution to the total amount of drag force on the blood vessel; thus, the net drag force is effectively given by the net efflux term.

Stent graft model. A stent-graft template was first defined on the basis of contrast-enhanced transaxial thoracic CT scan images of a patient. A cubic spline curve was fitted through the luminal cross sections, and the centerline was determined and used as a subsequent template for generating stent graft models of varying parameters. To limit the complexity, we assumed this initial model was non-tapering and without out-of-plane bending. Each model is generated as a smooth circular tube surface with the software Rhinoceros (Robert McNeel & Associates, Seattle, Wash) (Fig 2).

A stent-graft model in the form of the mesh elements was then generated, and the IGES format geometry files were then imported into a program ICEM CFX (Ansys Inc, Canonsburg, Pa) for surface mesh generation. A large number of elements and mesh smoothing are required to generate a sufficiently smooth surface and avoid sharp corners. Simulations of CFD are then performed on each stent-graft model according to its geometric parameters, and the governing equations and the boundary conditions. To solve these equations, we used the computational fluid dynamics code CFX, which is a finite volume method solver. Repeated calculations with finer meshes revealed the mesh independence of the results. More than 700,000 elements were created in the fluid domain for each model to achieve mesh independence.

Three geometric parameters were specified and studied in these idealized stent-graft models (Fig 2): the lumen (or stent graft) diameter, d; the starting position of the stent graft on the aorta, θ; and the diameter of curvature of the aortic arch, D. The starting position is defined by the proximal end of the graft and ranges from 0 to 180 degrees. The diameter of curvature of the aortic arch is the maximum horizontal distance between the centroids of the cross sections at the aortic arch. A standard stent graft length of 150 mm was used.

The relationship of the drag force with variations in the stent graft geometry was studied by applying the CFD simulations to different parameters of d (graft diameter), θ (graft position), and D (arch curvature). The graft diameter d studied ranged from 26 to 42 mm, graft position θ from 90 to 180 degrees, and arch curvature D from 70 to 130 mm. With each parameter being varied, the other two were fixed at their average values, assuming a constant value of d = 34 mm, θ = 90 degrees, and D = 100 mm.

Patient-derived models. Twelve patients with uncomplicated Stanford type B dissections treated by primary endovascular thoracic aortic stent grafting and who were followed up for at least 12 months were then chosen for this study. Of the 12 patients, 11 were men and one was a woman, with a mean age of 56 years (range, 31-78 years). Two were treated for acute dissection, seven were in the subacute (less than 1-month) stage, and three were at a more chronic stage with aneurysmal changes. The stent grafts used were Zenith TX2 proximal endograft compo-

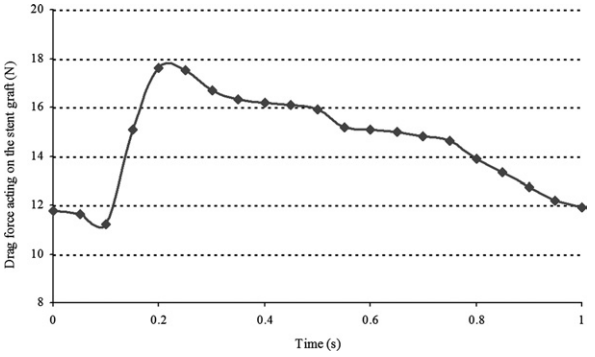

Fig 4. Relationship between the drag force acting on the stent graft and the cardiac cycle.

nents (Cook Medical, Bloomington, Ind). The landing zones were all close to the left subclavian artery origin. The landing zone aortic diameter averaged 32.8 mm (range, 28-38 mm), and the graft diameter averaged 37 mm (range, 34-42 mm), with a mean oversizing of 12.8% (range, 5%-31%). The average graft length was 153 mm. Contrast CT scans were routinely performed postoperatively and every 3 to 6 months thereafter.

For each patient, the geometry of the stent graft in the thoracic aorta was defined on the basis of CT transaxial DICOM images. The earliest postoperative scan and the latest scan images (a and b) were used for this analysis; the mean interval between the two scans was 16.3 months (range, 12-27 months). The CT scans gave a resolution of 512 by 512 pixels, with a pixel size of 0.625 mm and a slice thickness of 1.25 mm. The boundaries of the stent graft were readily segmented for the entire set of CT images. The software program SURFdriver (Moody and Lozanoff, Alberta, Calif), a surface reconstruction application, was used to segment the stent graft semiautomatically and then the polygon models were reconstructed by the rendering engine. The polygon models were used as input to the Rhinoceros software program (Robert McNeel & Associates, Seattle, Wash) and lofted into 3D nonuniform rational B-spline surfaces. The stent graft models in the form of the mesh elements were then generated. The IGES format geometry files of the stent graft model were produced and then input into ICEM CFX (Ansys Inc, Canonsburg, Pa) for surface mesh generation. Then, CFD simulation was performed on each stent graft model according to its geometric parameters, and the governing equations and the boundary conditions as described previously (Fig 3). Changes in stent graft inlet and outlet diameters were measured. Because axial sections of stent grafts are seldom circular, we expressed the stent graft size in terms of inlet ($A1$) and outlet ($A2$) cross-sectional areas. Comparisons were made by using the two-tailed paired samples t test. The changes in drag force (Fb/Fa) were correlated to the changes in inlet and outlet areas ($A1b/A1a$ and $A2b/A2a$) by using the Pearson correlation with two-tailed significance.

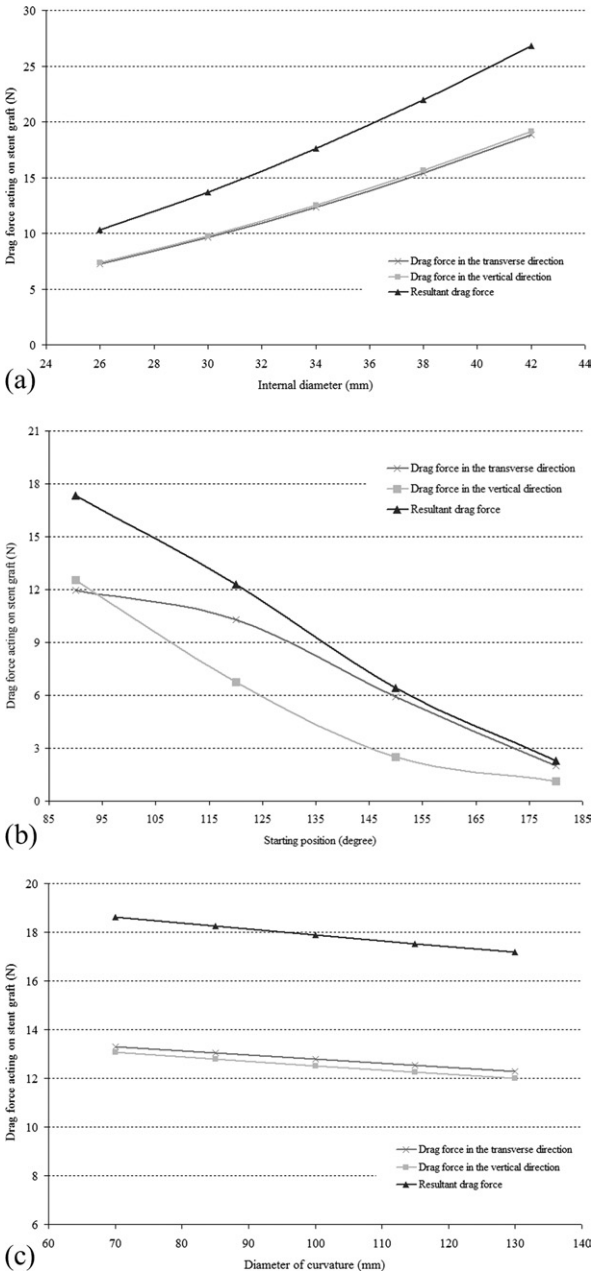

Fig 5. Relationship between the drag force due to net momentum change and the internal diameter of the thoracic stent graft (d) **(a)**, the deployment position of the thoracic stent graft (θ) **(b)**, and the diameter of curvature of the aortic arch (D) **(c)**.

RESULTS

Drag forces and cardiac cycle. The derived drag forces are generally related to the pressure changes in the cardiac cycle. A time-dependent plot of drag forces in a representative stent graft model (d = 34 mm and D = 100 mm) is shown in Fig 4.

Drag forces and stent graft geometry. On the simple geometry CFD simulation models, the drag forces in the

Table. Geometric and computational fluid dynamic data of 12 patients with thoracic aortic endografts

Patient	*Gender/ age (y)*	*Graft diameter (mm)*	*Inlet area 1 (mm^2)*	*Inlet area 2 (mm^2)*	*Outlet area 1 (mm^2)*	*Outlet area 2 (mm^2)*	*Inlet area change*	*Outlet area change*	*Inlet: outlet ratio 1*	*Inlet: outlet ratio 2*	*Drag force 1 (N)*	*Drag force 2 (N)*	*Drag force change*
CNW	M/53	34	891	832	635	985	0.93	1.55	1.40	0.84	19.87	23.33	1.17
FKM	M/67	42	871	1039	927	1372	1.19	1.48	0.94	0.76	18.34	24.19	1.32
WKC	M/58	42	967	1392	411	1707	1.44	4.15	2.35	0.82	16.07	26.24	1.63
CFC	M/55	34	799	726	413	638	0.91	1.54	1.93	1.14	16.32	18.11	1.11
CKF	M/58	34	1306	1298	685	736	0.99	1.07	1.91	1.76	26.18	30.18	1.15
KHW	F/78	38	832	835	304	256	1.00	0.84	2.74	3.26	23.38	25.17	1.08
KIC	M/31	34	1349	1598	576	767	1.18	1.33	2.34	2.08	21.59	23.11	1.07
KMC	M/57	36	958	1000	781	848	1.04	1.09	1.23	1.18	19.68	21.98	1.12
KPW	M/51	40	1048	1174	632	901	1.12	1.43	1.66	1.30	20.73	24.50	1.18
KWL	M/56	38	1023	1431	543	927	1.40	1.71	1.88	1.54	21.80	30.63	1.41
YYK	M/58	34	828	973	713	821	1.18	1.15	1.16	1.19	20.42	23.28	1.14
SAU	M/51	38	1484	1376	413	649	0.93	1.57	3.59	2.12	27.73	26.73	0.96

1, Initial postoperative scan measurements; *2*, follow-up scan measurements; *N*, Newtons.

transverse and vertical directions increased with the internal diameter of the graft (Fig 5, *a*). The resultant force on the thoracic stent graft is significantly larger than that experienced by its abdominal counterpart, and measured 10.3 N when the graft diameter was 26 mm and increased to 26.8 N with a graft diameter of 42 mm. The frictional force exerted on the blood vessel by the fluid contributes 0.036 N, which is less than 0.5% of the total drag force. Forces due to shear stress or friction thus appear to be negligible.

The relationship of the stent-graft landing position to the drag forces is shown in Fig 5, *b*. The force is greatest at the 90-degree position (top of the arch) and decreases significantly when the proximal landing zone is in the descending aorta (17.3 N at 90 degrees, 2.3 N at 180 degrees).

There is a slight decrease in drag force when the curvature of the thoracic aorta increases. The rate of change of the drag force in relation to the diameter of curvature of the aortic arch however is small (Fig 5, *c*). There is only an 8% reduction in resultant forces when the diameter changes from 70 to 130 mm.

Stent graft remodeling in aortic dissections. Serial CT scans of patients showed that, after endovascular stent-graft placement for aortic dissections, there was a general increase in both inlet and outlet graft areas (Table, Fig 6, *a* and *b*). An increase in mean inlet area was observed in eight patients; the area changed from 1030 ± 228 mm^2 to 1140 ± 279 mm^2 (increase of 11%; $P = .05$). There was a more marked (58%) increase in the mean distal outlet area, which was evident in all but one patient, with a resultant change of 586 ± 180 mm^2 to 884 ± 367 mm^2 ($P = .01$; Table). The general shape of the stent grafts remains conical with a larger inlet area, although the inlet:outlet area ratio decreased from a mean of 1.93 (range, 0.94-3.59) to 1.50 (range, 0.76-3.26). In three patients the outlet diameter of the graft had exceeded the inlet area. There was no relationship with the timing of the dissection and the remodeling changes.

A general trend of increasing drag force with larger-diameter stent grafts was observed.

In association with graft expansion, the CFD models showed an increase in resultant drag force on the stent graft in all but one patient (Fig 6, *c*). The mean drag force increased from 21.0 ± 3.5 N to 24.8 ± 3.4 N (mean increase, 19.5%; range, −4% to 63.2%; $P = .002$). There is a positive relationship between increase in drag force and increase in stent-graft outlet area ($P < .05$, Pearson correlation).

DISCUSSION

Stent grafts placed in the thoracic aorta near the arch are subjected to considerable pressure and flow, but no previous study has addressed the hemodynamic forces acting on thoracic aortic stent grafts. To date, CFD studies on aortic stent grafts have been performed on only bifurcated abdominal graft models. In a simplified, non-pulsatile, steady-state uniform flow CFD model, Liffman et al[1] have demonstrated that forces on abdominal stent grafts are related to graft inlet diameter in the order of 3 to 5 N for small grafts and 7 to 9 N for larger grafts. A recent study using 3D non–steady-state CFD analysis on CT-defined models by the Stanford group[2] showed similar force magnitudes; the study also verified that pressure-related forces were much larger than flow-related forces in abdominal stent grafts, and that blood pressure, inlet graft diameter, and angulation were the determining factors. These studies also confirmed that forces on abdominal grafts act mainly on the bifurcation and thus implied that tube-shaped thoracic grafts should be more stable.

We used actual 3D, pulsatile flow mechanics to produce a more realistic CFD model. The pressure and velocity waves were verified by using in vivo arterial pressure measurements. This CFD model has been tested on a simulated abdominal bifurcated graft environment, and the outcome was in agreement with previous findings. We have demonstrated that the drag forces acting on the thoracic stent grafts were of a significantly higher magnitude than the abdominal counterparts, averaging 10 N for the smallest diameter grafts and reaching 26 N for grafts with a 42-mm diameter at the aortic arch. These forces were in an almost

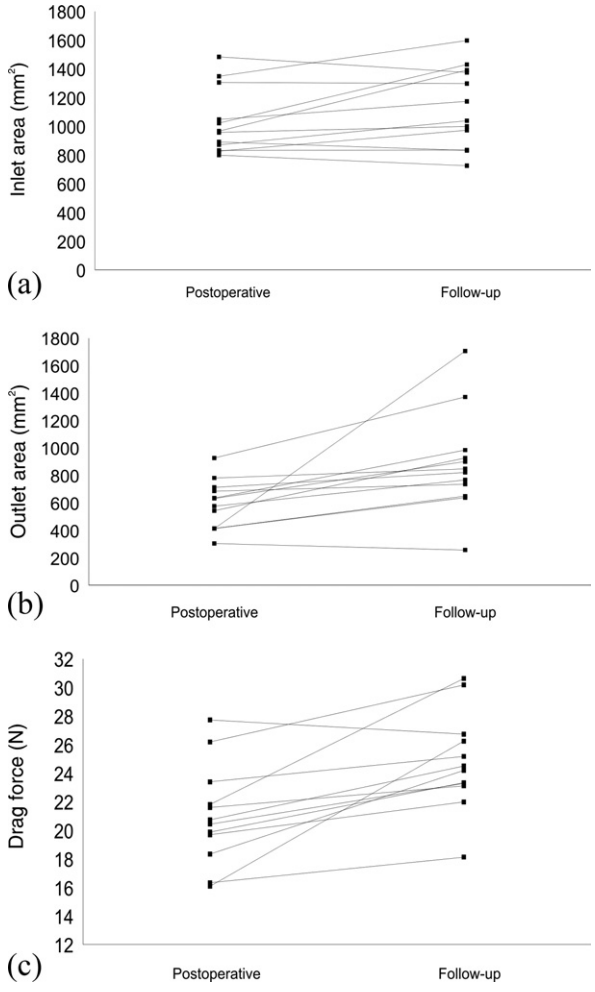

Fig 6. Changes in the inlet area (**a**), the outlet area (**b**), and the drag force of the thoracic stent grafts (**c**).

linear relationship with the diameter of the graft; a large-diameter graft is subjected to a higher displacement force. We have also shown that drag forces on thoracic stent grafts arise primarily from shifts in fluid momentum as a result of pressure and flow changes. Shear stress, the frictional forces between blood and the luminal surface, was two orders smaller. The effect of contact surface (and therefore the length) of the graft appears to be negligible.

The deployment position of the stent graft also has a significant bearing on resultant drag forces. A 34-mm graft deployed at the top of the arch experiences forces of 17 N compared with only 2 N when it is deployed at 180 degrees. Stent grafts that are placed in a proximal position must experience an additional transverse displacement force. This force may explain the significant increase in the resultant distraction forces of thoracic stent grafts placed in the curved part of the arch compared with a significantly smaller force on the straight part of the descending thoracic aorta.

Drag forces are counteracted by fixation forces from the stent graft, mainly frictional forces from the stents, and hooks and barbs at the proximal end. In bench top experiments, a force of 10 to 25 N is required to displace an abdominal endograft with suprarenal fixation,[8,11] and more than 30 N is required for fenestrated grafts.[11] In vivo experiences also suggested that graft diameter is a significant determinant of migration.[12] There is no study on in vitro displacement forces of thoracic stent grafts. The drag force computations in this study in horizontal and vertical directions are the forces acting on the stent graft in isolation, and are only an estimation of one of many factors that may lead to stent graft migration in real life. Only an unknown portion of the total drag force estimated in our computations will be parallel to the attachment site. An additional counterbalancing force by stent graft contact and fixation hooks exists to oppose these drag forces on the graft.[13] The choice of the length of thoracic stent grafts is more flexible, and a longer distal landing zone is often used, which may account for greater stability. The addition of a series of bare metal stents in the distal aorta as advocated by some centers may also help to maintain the position of the stent graft.

Although device migration is a known complication of thoracic stent grafts, there is very little long-term data on thoracic endograft migration. The Gore TAG registry on thoracic aneurysms reported a total migration rate of 10% at 2 years.[14] The Cook Zenith TX2 trial registered a device migration rate of 2.8% at 12 months.[15] A study using the computer centerline of flow measurements in 194 patients recorded migration in 6.7% of thoracic devices.[16] These studies were performed on stent grafts for thoracic aneurysms; data on aortic dissections are lacking at this point in time.

Type B aortic dissection is now increasingly being treated by endovascular repair in which a short- to medium-length stent graft is used to cover the primary entry tear. Because of the anatomic proximity of the primary tear to the major branches of the arch, the proximal landing zone is often short and on less healthy tissue. Liberal oversizing at the top is not advisable for fear of iatrogenic dissections; it also reduces the proximal fixation force even more. The distal landing is typically in the diseased true lumen of a dissected aorta, with the majority of the stent grafts held against the dissection flap rather than a healthy aortic segment. After successful exclusion of the false lumen, there is a progressive dilatation of the true lumen with time attributable to realignment of the blood flow. A continuing, gradual expansion of the stent graft is usually observed on follow-up. Patients with aortic dissections are usually younger (the mean age of patients in our study was 56 years), and their aortas are more compliant and prone to dilation in future. The drag force on the stent graft may change with time and may not reach a steady state until many months after graft implantation.

We have shown that substantial remodeling of the stent graft existed in patients with aortic dissections. Progressive dilatation of both the proximal and distal lumens occurred,

but was more marked for the latter. As the false lumen thromboses and regresses, the true lumen will gradually expand, whereas the proximal portion of the stent graft is constrained by a healthy aorta at the landing zone, resulting in a shape change of the graft from a more conical configuration to a more cylindrical appearance. Associated with these changes was an increase in hemodynamic drag forces, amounting to almost 20%, and in some of the cases exceeding 60%. These changes must be related to the remodeling of the stent graft configuration. Existing in a dynamic state, these thoracic stent grafts are at the highest risk of subsequent migration. Paradoxically excessive oversizing of a stent graft will result in further distal dilatation and a more significant rise in drag forces with time. Stent grafts composed of Gianturco Z-stent elements may also exhibit a gradual decrease in radial expansion force as the stent increases in diameter.

This study is subjected to the standard limitations of CFD analysis, and several assumptions were made to limit the complexity of the model calculations. In the initial geometry model, the stent grafts were built as cylindrical tubes without 3D twists and the inlet was axis symmetrical. The stent graft is viewed as a rigid, non-pulsatile tube, but in reality pulsations have been observed in stent graft elements. In a recent study[17] using dynamic CT angiography, changes in thoracic stent graft diameter of up to 5 mm with aortic pulsatility were reported. In aortic dissection there are more propensities for movement, because the dissection flap moves with pressure. The experience of treating aortic dissection with stent grafts is still relatively new, and only time will tell whether these grafts will be less durable than other thoracic repairs.

CONCLUSION

Using 3D pulsatile flow CFD techniques, we have shown that the drag force on a thoracic stent graft is high, and that it is dependent on the graft diameter and the deployment position. In aortic dissections, consideration must be given to drag force changes, because significant graft diameter remodeling was evident.

AUTHOR CONTRIBUTIONS

Conception and design: SC, KC
Analysis and interpretation: SC, EL, GF
Data collection: SC, PH, AT
Writing the article: SC, EL
Critical revision of the article: SC, EL
Final approval of the article: SC
Statistical analysis: SC
Obtained funding: SC, KC
Overall responsibility: SC

REFERENCES

1. Liffman K, Lawrence-Brown MM, Se mmens JB, Bui A, Rudman M, Hartley DE. Analytical modeling and numerical simulation of forces in an endoluminal graft. J Endovasc Ther 2001;8:358-71.
2. Howell BA, Kim T, Cheer A, Dwyer H, Saloner D, Chuter TA. Computational fluid dynamics within bifurcated abdominal aortic stent-grafts. J Endovasc Ther 2007;14:138-43.
3. Kim T, Cheer AY, Dwyer HA. A simulated dye method for flow visualization with a computational model for blood flow. J Biomech 2004;37:1125-36.
4. Nichols WW. McDonald's blood flow in arteries : theoretical, experimental, and clinical principles. 4th ed. London: Arnold/Oxford University Press; 1998.
5. Pedley TJ. Mathematical modelling of arterial fluid dynamics. J Eng Math 2003;47:419-44.
6. Fung YC. Biomechanics: circulation. 2nd ed. New York: Springer; 1997.
7. Morris L, Delassus P, Walsh M, McGloughlin T. A mathematical model to predict the in vivo pulsatile drag forces acting on bifurcated stent grafts used in endovascular treatment of AAA. J Biomech 2004;37: 1087-95.
8. Resch T, Malina M, Lindblad B, Malina J, Brunkwall J, Ivancev K. The impact of stent design on proximal stent-graft fixation in the abdominal aorta: an experimental study. Eur J Vasc Endovasc Surg 2000;20:190-5.
9. Shahcheraghi N, Dwyer HA, Cheer AY, Barakat AI, Rutaganira T. Unsteady and three-dimensional simulation of blood flow in the human aortic arch. J Biomech Eng 2002;124:378-87.
10. Franzini JB. Fluid mechanics with engineering applications. New York: McGraw-Hill; 1997.
11. Zhou SS, How TV, Rao Vallabhaneni S, Gilling-Smith GL, Brennan JA, Harris PL, et al. Comparison of the fixation strength of standard and fenestrated stent-grafts for endovascular abdominal aortic aneurysm repair. J Endovasc Ther 2007;14:168-75.
12. Mohan IV, Harris PL, Van Marrewijk CJ, Laheij RJ, How TV. Factors and forces influencing stent-graft migration after endovascular aortic aneurysm repair. J Endovasc Ther 2002;9:748-55.
13. Malina M, Lindblad B, Ivancev K, Lindh M, Malina J, Brunkwall J. Endovascular AAA exclusion: will stents with hooks and barbs prevent stent-graft migration? J Endovasc Surg 1998;5:310-7.
14. Makaroun MS, Dillavou ED, Kee ST, Sicard G, Chaikof E, Bavaria J, et al. Endovascular treatment of thoracic aneurysms: results of the phase II multicenter trial of the GORE TAG thoracic endoprosthesis. J Vasc Surg 2005;41:1-9.
15. Matsumura JS, Cambria RP, Dake MD, Moore RD, Svensson LG, Snyder S. International controlled clinical trial of thoracic endovascular aneurysm repair with the Zenith TX2 endovascular graft: 1-year results. J Vasc Surg 2008;47:247-57.
16. O'Neill S, Greenberg RK, Resch T, Bathurst S, Fleming D, Kashyap V, et al. An evaluation of centerline of flow measurement techniques to assess migration after thoracic endovascular aneurysm repair. J Vasc Surg 2006;43:1103-10.
17. Muhs BE, Vincken KL, van Prehn J, Stone MKC, Bartels LW, Prokop M, et al. Dynamic Cine-CT angiography for the evaluation of the thoracic aorta; in sight in dynamic changes with implications for thoracic endograft treatment. Eur J Vasc Endovasc Surg 2006;32:532-6.

Submitted Dec 12, 2007; accepted Mar 27, 2008.

DISCUSSION

DR. STARNES: Chairman, ladies and gentlemen. At first glance, computational fluid dynamic analysis of the forces exerted upon stent grafts seems a bit challenging and daunting in terms of the complex physics equations involved. Dr. Cheng and his colleagues, however, have taken a simplistic approach to the measurement of forces exerted upon stent grafts in the thoracic location. More specifically, they have attempted to characterize the forces exerted in a dissection model by introducing CT measurements pre and post endovascular management of aortic dissection.

The authors have provided us with some valuable information. Namely, that, (1) the drag forces exerted upon stent grafts in the thoracic location increase dramatically with increasing diameter. In this study an increase in graft diameter of 62%, that is, from 26 mm to 42 mm, correlated with an increase in drag forces of 160%, with the highest calculated drag force in this series being 30 N, which is fivefold higher than the mean force exerted upon infrarenal bifurcated grafts; (2) the mere presence of curvature matters more than the degree of curvature. Stated more plainly, substantial drag force is exerted on a graft placed transversely in the arch versus those placed in a rather straight portion within the descending aorta; and (3) stent graft length has minimal impact on the drag force exerted within the stent graft.

I have the following three series of questions for the authors:

Number one, your analysis was based on CT scans of 12 actual patients presenting with uncomplicated type B aortic dissections. Can you tell us more about these patients? What was the vintage of the aortic dissections? We know that the septa tend to be leather-like in chronic dissections. Were these all acute or a mixture of acute and chronic? And how did the age of the dissection affect drag force and aortic remodeling? More importantly, in followup of at least 12 months, how many of the patients actually demonstrated migration and did this correlate as you suggest, with drag force?

Number two, currently the only stent graft in the US approved by the FDA for implantation in the thoracic aorta is the WL Gore TAG endoprosthesis. All of your thoracic stent grafts were Cook TX2's that have positive fixation in the form of barbs. In your opinion, is positive fixation mandatory in the thoracic region based on the momentum forces that you have shown to be exerted upon these grafts?

And finally, this brings up the issue of managing uncomplicated type B aortic dissections. Are we to understand that you manage all dissections with an endovascular approach? Current literature suggests that roughly 30% of type B dissections progress to aneurysmal degeneration; however, in our series we have observed a smaller number to progress and the majority of these patients have a benign clinical course with medical management alone. What is your rationale for treating these patients?

I would like to thank the authors again for an elegant manuscript and fine presentation and the Society for the opportunity to discuss this paper.

DR. CHENG: Thank you very much, Ben, for the very insightful comments.

The patients were a mix between acute, subacute and chronic dissections. These represent our earliest experiences with a series of patients with more than 12 months of followup. I believe 7 endografts were performed in the subacute stage meaning that they are done within one month of the dissection, 2 patients were treated in the acute stage, and 3 patients for dissecting aneurysms. It is not within the confines of this study to investigate the relationship of remodeling and the age of the dissecting flap and we have found no correlation between the timing of the procedure and remodeling in our series.

Two of our patients had shown some degree of stent graft migration over the length of the followup period with one significantly. It may be a coincidence that both of these patients had very large diameter grafts placed in their aorta – both were 42–mm grafts. However, the position of the stent graft on the aorta is dependent on the drag forces as well as the fixation forces. The fixation forces are determined by a lot of variables like the length and the health of the landing zone, and graft oversizing, the length of the stent graft which provides friction, and whether there is any distal attachment or bare stents. Without looking at these fixation forces we cannot comment on whether the migration is a result of increasing drag forces. It is also possible that an increase in migration of the stent graft could result in an actual expansion of the diameter of the graft and therefore further increase in the drag forces, but these are all speculations.

Our experience is mainly with the Cook TX2 graft. I believe previous bench top studies on abdominal grafts have shown that the grafts with hooks and suprarenal fixation would be able to sustain a higher distraction force. I believe the distraction force required to dislodge an abdominal graft is in the order of 24 N. Since the result of this study showed that there is a significantly higher drag force in the aortic arch, I believe the use of added fixation is certainly highly desirable.

Concerning the indication of treating patients with type B dissection, I believe that it is still controversial. We certainly do not treat all the patients with endovascular stent grafting. In acute situations, we only treat patients with branch vessel compromise and end organ ischemia or in a patient with severe pain. In subacute situations we would offer this to patients when the aortic false lumen remained patent, especially if the aortic diameter exceeded 4 cm. We do this in 3 to 4 weeks. In a chronic situation we only do aneurysms. We will not treat a chronic stable type B dissection.